SKIN OF *ALLIUM SATIVUM* (GARLIC) MEDIATED GREEN SYNTHESIS OF ZnO NANOPARTICLES AND IT'S ADSORPTION PERFORMANCE FOR CONGO RED DYE REMOVAL: KINETIC, ISOTHERM AND THERMODYNAMIC STUDIES

Bandela Sowjanya[1], Pulipati King[2], and Meena Vangalapati[3*]

.

Abstract

This study attempts to use Skin of *Allium sativum*(Garlic) to the green synthesis of Skin of *Allium sativum*/zinc oxide nanoparticles as an adsorbent to remove Congo red, a toxic azo dye, from an aqueous solution. XRD, SEM, and FTIR tests were performed to determine the particles' characteristics. For the adsorption process, the ideal values for the process variables agitation time, adsorbent dosage, pH, initial dye solution concentration, and temperature were identified. The maximal adsorption capacity of synthesised Skin of *Allium sativum*/zinc oxide nanoparticles is 105.75 mg/g.

Keywords: Green Synthesis, *Allium Sativum*, Zinc Oxide, Nanoparticles, Congo red

[1,2,3*]Department of Chemical Engineering, AUCE, Visakhapatnam, AP, India.

***Corresponding Author:-** Bandela Sowjanya
[*]Department of Chemical Engineering, AUCE, Visakhapatnam, AP, India.

DOI: - 10.31838/ecb/2023.12.si5.039

1. Introduction

Polluted water contains a variety of contaminants, including harmful heavy metals, organic pollutants including dyes, pesticides, and medicines, degraded organic materials, etc. [1]. In addition to being harmful, dyes among these contaminants can alter the colour of the water. This can lessen the photosynthetic reaction and have an impact on the aquatic biota since it diminishes or entirely blocks sunlight from entering the stream. The most hazardous dyes are those with one or more azo bonds (-N=N-), which might be anionic, cationic, or non-ionic in nature. A major class of anionic azo dyes with aromatic rings and one or more azo linkages have been shown to have extremely high stability and biodegradability. One such anionic dye, Congo Red (CR), comprises the non-degradable aromatic groups benzidine and biphenyl and napthalene. The chemical compound CR has a molecular mass of 696.66 g/mol and the molecular formula $C_{32}H_{22}N_6Na_2O_6S_2$ of benzidinediazo-bis-I-naphthylamine-4-sulfonic acid. [2].

Adsorption, coagulation/flocculation, electroche-mistry, photocatalysis, ion exchange, and microbial degradation, both aerobic and anaerobic, are common methods for eliminating dyes from wastewater. Adsorption is the most practical and advantageous of these methods due to its uncomplicated operation, high efficacy, and low energy demand [3]. A good adsorbent should have a large surface area, be porous, and behave non-toxically because these qualities are essential for removing dyes. A number of conventional adsorbents have been investigated, including activated carbon, clay minerals, silicon nanoparticles, and metal oxides [4].

Because of the development of new functional nanomaterials that are highly effective at removing different types of pollutants from water, the application of nanotechnology for water remediation has recently attracted more attention. Nanomaterials can be created using a variety of processes, including sol-gel, hydrothermal, laser induced, ultrasonic, thermal decomposition, precipitation, and more. Their sizes range from 1 to 100 nm [1]. Nanomaterials have a very large surface area due to their incredibly small size, which increases the contact between dirty water and the nanomaterials. The efficacy of the nanomaterial's adsorption toward different contaminants is boosted by the increased contact. Green approaches allow for the large-scale synthesis of pure ZnO-NPs free of any impurities while also being economical, cost-effective, biocompatible, and safe. Several plant extracts, including fresh or dried leaves, rhizomes, flowers, and fruits, could be used to synthesise ZnO NPs. In the current investigation, Skin of *Allium sativum*/Zinc Oxide nanoparticles (A.Sa/ZnO-NPs) were created using the co-precipitation approach. FTIR, SEM, and XRD techniques were used to characterise the produced samples.

2. Materials and Methods

2.1Materials

Skin of *Allium sativum* (Garlic) was obtained from local market, Visakhapatnam, A.P, India. $ZnSO_4$ $7H_2O$, NaOH, Congo Red (CR) were purchased from Lotus chemicals private limited, Visakhapatnam, A.P, India.

2.2. Preparation of skin of Allium sativum extract:

The skin of garlic were collected from the vegetable market, cleaned with distilled water and are properly dried in sun and after that they are grinded into fine powder. 40g of skin of *Allium Sativum* powder is mixed with 500ml distilled water at 90°C for 40 mins. After the mixture is cooled, it is then filtered using filter paper. The filtered solution is the required skin of *Allium Sativum* extract.

2.3 Green Synthesis Of Skin of *Allium Sativa/ZnO Nanoparticles (A.Sa/ZnO-NPs)*

0.1M zinc sulphate ($ZnSO4.7H_2O$) solution is synthesized by mixing 14.4g of zinc sulphate hexahydrate with 500ml of distilled water. The pH of the mixture was kept at 8 to produce smaller-sized particles. 100ml of skin of *Allium Sativum* extract is added to the 500ml of zinc sulphate solution, and the mixture is agitated for three hours at room temperature using a stirrer [5]. For 20 minutes, the solution was centrifuged at 3600 rpm; the supernatant was then discarded, and the sediment was collected. The obtained sample was then dried in a 100°C oven and ground into a powder using a mortar and pestle before being placed in an airtight container for further examination (fig.1) [6].

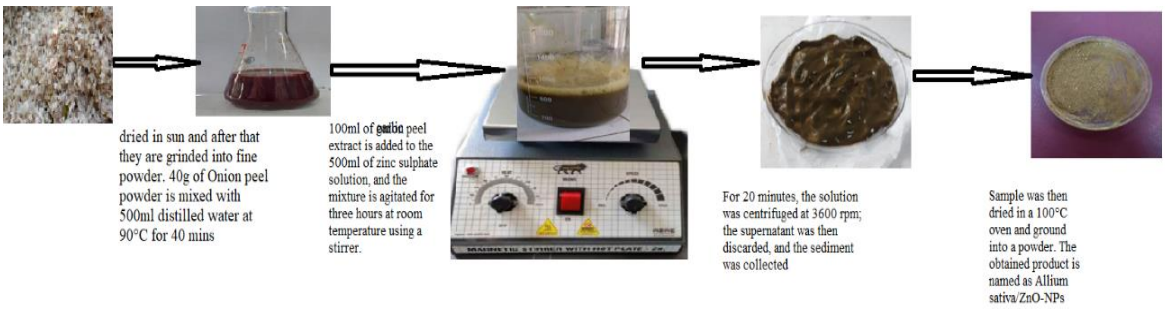

Figure 1. Synthesis Procedure for skin of *Allium Sativum*/ZnO-NPs

2.4 Batch Adsorption Experiments

Adsorption tests involved adjusting the agitation time (in minutes), adsorbent dosage (g/L), pH, temperature (Kelvin), and initial concentrations (mg/L). The current investigation tested the effects of agitation time (5 to 60 min), adsorbent dosage (0.1to 0.8 g/L), pH (4 to 9), temperature (308, 313, 318, 323 and 328 K), and initial CR dye concentration (10 to 100 mg/L) [7].

2.5 Adsorption isotherms, kinetics and thermodynamics

Adsorption equilibrium tests show the adsorbent's effectiveness. Since monolayer sorption onto a surface with a finite number of identical sites is acceptable, the Langmuir equation is the isotherm equation that is most usually employed to represent the adsorption data. The Freundlich isotherm provides an explanation for the heterogeneous nature of adsorption sites with non-uniform energy level distribution [7]. Using models of pseudo-first-order and pseudo-second-order, adsorption

kinetics were studied. Three thermodynamic parameters related to adsorption are standard free energy change (△G), standard enthalpy change (△H), and standard entropy change (△S). The equation yields the free energy of the sorption process [4] after accounting for the distribution coefficient K_c.

2.6 A.Sa/ZnO-NPs *characterization*

XRD analysis. The peaks are 14.560, 19.530, 27.140, 31.350, 37.810, and 43.560 in order of elevation (Fig.2. (a)). All of the sample's diffraction peaks are consistent with the distinctive hexagonal wurtzite structure of A.Sa/ZnO NPs. The Debye-Scherrer equation's mathematical computation showed that the produced A.Sa/ZnO NPs are smaller than 100 nm in size. Further evidence that the produced A.Sa/ZnO NPs are pure crystals comes from the XRD special pattern [8].

SEM analysis. The surface morphology of the sample is seen in the SEM image in Fig. 2(b). As per Fig. 2(b), the substance has a permeable surface & agglomerated particles. According to a SEM study, dyes can access both broad and microscopic pockets on A.Sa/ZnO nanoparticles' surfaces to interact with their surface atoms [7].

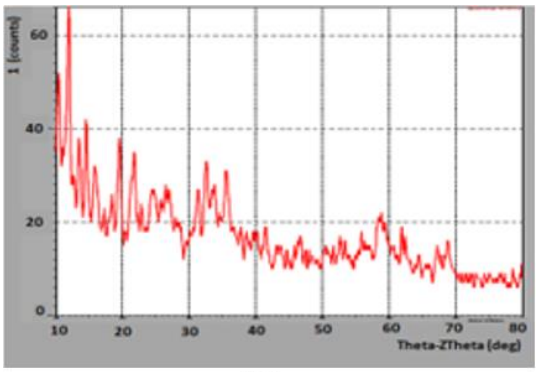

(a)

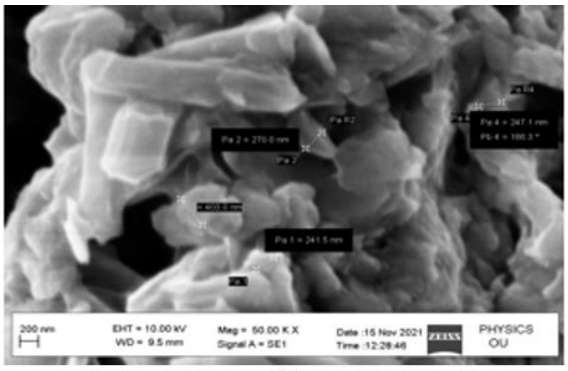

(b)

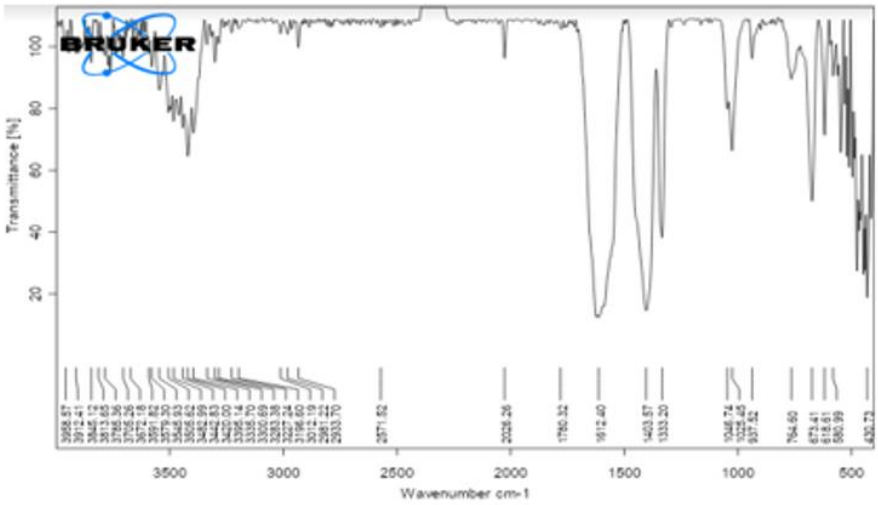

(c)

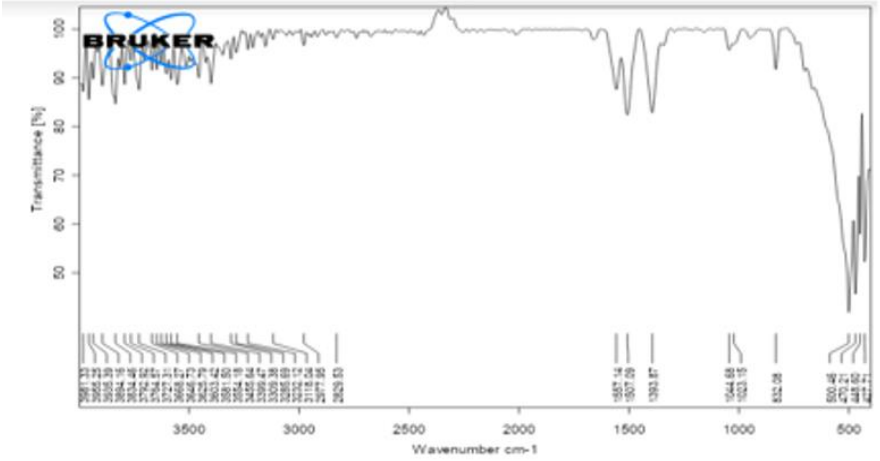

(d)

Figure 2 Skin of *Allium Sativa*/ZnO-NPs characterization (a) XRD (b) SEM (c) FT-IR spectra of A.Sa/ZnO-NPs, (d) FT-IR spectra of A.Sa/ZnO-NPs after adsorption of CR.

3. Results and discussion

3.1 FT-IR

A more thorough investigation of the adsorption mechanism was conducted using FT-IR. The results of the FT-IR of A.Sa/ZnO-NPs are shown in fig. 2(c). Figure 2(d) shows the FT-IR spectra of CR-loaded A.Sa/ZnO-NPs. The peaks are detected at 1044 cm^{-1} because C-N of CR dye is present. The broadening of the strong peak at 1612 cm^{-1} following adsorption demonstrated the association of the CR dye with the A.Sa/ZnO-NPs.

3.2 A.Sa/ZnO-NPs for adsorption of CR dye

Effect of agitation time. Within 30 minutes of the reaction with adsorbent, the maximal removal of dye was achieved (fig. 3(a)). However, the percentage of CR removal was found to be 45 percent after only 5 minutes, and it progressively increased to 61.4 percent over the next 30 minutes. These results demonstrate that the rate of adsorbent removal ascending with increasing agitation period and achieves steadiness within 30 minutes, but beyond that, the rate of removal almost stays constant. This outcome might be due to the CR dye molecules being able to adsorb on a lot of surface area for the first 30 minutes, followed by the saturation of the unoccupied surface sites, which would retain the same removal efficiency [3].

Effect of different dosages of A.Sa/*ZnO-NPs.* Another very important component for removal process is the dosage of A.Sa/ZnO-NPs since it controls how much adsorbate can be absorbed by a specific mass of A.Sa/ZnO-NPs. Figure 3 illustrates how different dosages of A.Sa/ZnO-NPs (0.1, 0.2, 0.3, 0.4, 0.5, 0.6, 0.7, and 0.8 g/L) affect the adsorption of CR at 308K temperature (b). The decolorizing efficiency of A.Sa/ZnO-NPs improved from 36.6 percent to 61.4 percent when adsorbent dosage increased from 0.1g/L to 0.5g/L, but beyond 0.5 g/L the rate of removal remains almost steady. This was clearly seen in fig. 3(b).

The findings demonstrate that as adsorbent dose is raised, the quantity of active sites also rises, which can stimulate more CR dye molecules to bind to the A.Sa/ZnO-NPs surface and hasten the removal of the dye [1].

Effect of pH. According to Fig. 3(c), for basic solutions, the percent removal of CR decreases while the pH increases from 4 to 7. Lower pH causes the -NH_2 groups in CR to protonate and turn into -NH_3^+. As a result of the dye molecule having a positive charge, there is an attractive interface between the surface of ZnO and it, which causes percentage of CR dye removal to drop [4].

Effect of initial dye concentration. Figure 3(d) demonstrates that removal effectiveness falls as the starting concentration rises, demonstrating that A.Sa/ZnO-NPs lose their ability to absorb dye at greater concentrations. This might be because, in spite of the low dye concentration, the surface of A.Sa/ZnO-NPs possessed a significant number of active sites that were adequate to hold all of the dye molecules in the solution. Consequently, the quantity of active sites increases as dye solution concentration does.

*Effect of temperature***.** The removal efficiency improved as the temperature rose, as shown in Fig. 3(e). This result proved that the CR adsorption by A.Sa/ZnO-NPs was endothermic. As the temperature rises, dye molecules become more mobile and dispersed in liquids. More adsorption occurred at higher temperatures as a result of the dye molecule's faster rate of interaction with the adsorbent's active sites [10].

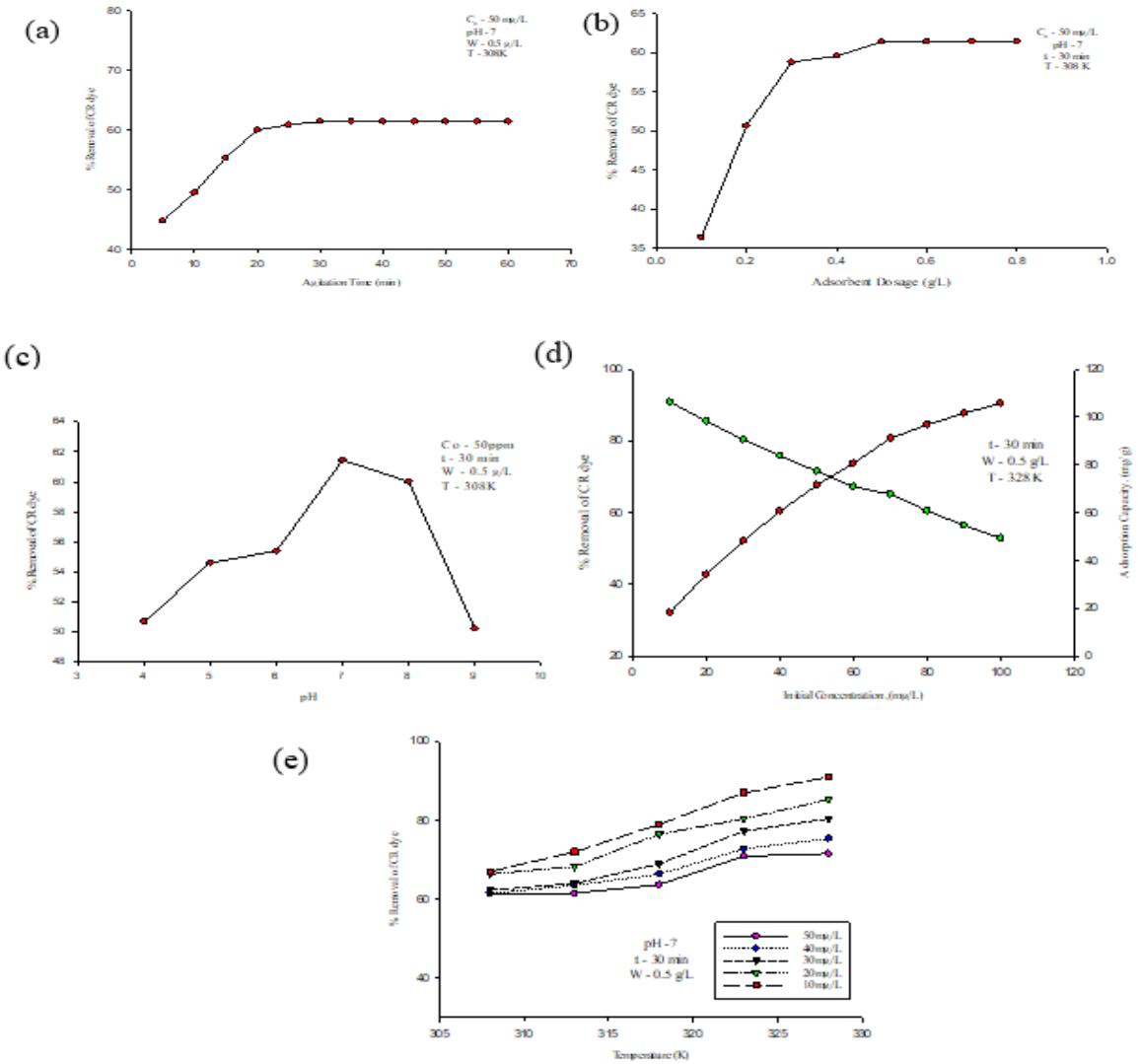

Figure 3 Removal effects of CR dye by Skin of *Allium Sativa*/ZnO-NPs (a) Agitation time, (b) Adsorbent dosage, (c) pH, (d) Initial Concentrations of CR dye (e) Temperature

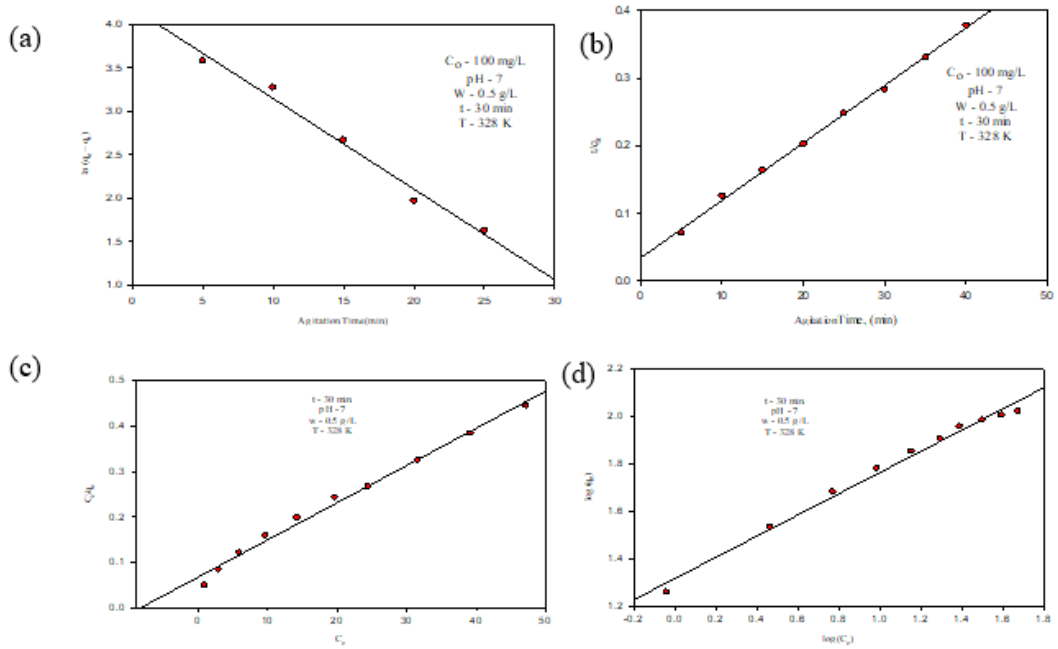

Figure 4 Kinetics, isotherms, thermodynamics of adsorption (a) Pseudo-first-order kinetics; (b) Pseudo-second-order kinetics; (c) Langmuir isotherm model; (d) Freundlich isotherm model;

3.3 Adsorption kinetics, isotherms and thermodynamics

The adsorption rate is thought to be proportional to the difference between q_e and q_t according to the pseudo-first-order model [11]. For pseudo-second-order, it is believed that the adsorption process is controlled by a chemical adsorption mechanism involving electron sharing or transfer of electrons between the adsorbent and the adsorbate [12]. In Figures 4(a) and 4(b), the plots of these kinetic models are displayed. Each model's accuracy is confirmed by the accompanying correlation coefficients (R^2). The method and rate of CR dye uptake on A.Sa/ZnO-NPs are best explained by the pseudo-second-order kinetic model, according to a comparison of the R^2 values of the kinetic models. The monolayer adsorption that occurs on the uniform adsorbent's outermost layer is best described by the Langmuir isotherm. In a variety of non-ideal situations, the Freundlich model is used to explain heterogeneous surface adsorption and multilayer adsorption [13]. Figures 4 (c) and 4 (d) provide fitting charts for these models. The adsorption data may be better explained by the Langmuir model, which has a higher correlation coefficient (R^2 = 0.9909) than the Freundlich model (R^2 = 0.988). The adsorption capacity, is 122.1 mg/g for CR dye, may be calculated using the Langmuir model. This figure matches the experiment's measured adsorption capacity fairly well [14, 15].

The thermodynamic parameters can be calculated using the results from the graph of lnKc vs 1/T. The adsorption process was spontaneous and physically feasible because ΔG was negative at various temperatures. As the temperature rises, the ΔG values slightly decline, which implies that at higher temperatures, more dye was adsorbed into the adsorbent surface. As a result, slightly higher temperatures are preferred for CR dye adsorption. The +ve values of ΔH and ΔS throughout the process demonstrate the endothermic nature [10, 16, 17].

4. Conclusion

Zinc oxide nanoparticles have been synthesized using the Skin of *Allium Sativa* extract, and they were successfully used to remove CR dye after being characterised using XRD, SEM, and FT-IR techniques. The best CR dye removal by A.Sa/ZnO-NPs was seen at agitation time of 30 min, adsorbent dosage of 0.5 g/L, initial CR concentration of 10 mg/L, and temperature of 328 K. The experimental, pseudo-second-order kinetics, and Langmuir isotherm adsorption capacities were 105.75 mg/g, 117.5 mg/g, and 122.1 mg/g, respectively. The adsorption process is endothermic and spontaneous, according to thermodynamic research. These findings imply that skin of *Allium Sativa*/ZnO- NPs may serve as an effective CR adsorbent. As a result, the work provides a method for the environmentally friendly synthesis of skin of *Allium Sativa*/ZnO NPs that is effective, inexpensive, easy, unique, safe, and convenient.

References:

1. Debnath, Priyanka, Mondal, Naba: Effective removal of congo red dye from aqueous solution using biosynthesized zinc oxide nanoparticles, Environmental Nanotechnology, Monitoring & Management. (2020).
2. Prachi Palai, Sthitiprajna Muduli, Barsharani Priyadarshini, Tapas Ranjan Sahoo: A facile green synthesis of ZnO nanoparticles and its adsorptive removal of Congo red dye from aqueous solution. Materials Today: Proceedings, 38 (5), 2445-2451 (2021).
3. Ansuman Nayak, Jitendra Kumar Sahoo, Shraban Kumar Sahoo & Duryodhan Sahu, Removal of congo red dye from aqueous solution using zinc oxide nanoparticles synthesised from *Ocimum sanctum* (Tulsi leaf): a green approach: International Journal of Environmental Analytical Chemistry. (2020).
4. Fan Zhang, Xin Chen, Fenghuang Wu, Yuefei Ji, High adsorption capability and selectivity of ZnO nanoparticles for dye removal, Colloids and Surfaces A: Physicochemical and Engineering Aspects, 509, 474-483 (2016).
5. Hanna Mariya Joseph, N. Poornima, Synthesis and characterization of ZnO nanoparticles: Materials Today: Proceedings. 9 (1), 7-12 (2019).
6. Mata Subhashita, Thanusha Punugoti, Bandela Sowjanya, Venkat Rao Poiba and Meena Vangalapati: Synthesis of Cu/ZnO nanoparticles and its exploitation as a catalyst for the removal of Cetrimonium Bromide. J. Advances in Materials and Processing Technologies (2021).
7. Bandela Sowjanya, U. Sirisha, Alpitha Suhasini Juttuka, Sreenivas Matla, Pulipati King, Meena Vangalapati: Synthesis and characterization of zinc oxide nanoparticles: It's application for the removal of alizarin red S dye. Materials Today: Proceedings 62(6), 3968-3972 (2022).
8. Dudekula Parveen, Venkata Rao Poiba & Meena Vangalapati: Characterisation and performance of ZnO nanoparticles for the removal of sodium dodycl sulphate. Advances in Materials and Processing Technologies, (2020).
9. Amit Kumar Chauhan, Navish Kataria, V.K. Garg: Green fabrication of ZnO nanoparticles using Eucalyptus spp. leaves extract and their application in wastewater remediation. Chemosphere, 247, (2020).
10. Kataria, Navish: Preparation, characterization and potential use of flower shaped Zinc oxide nanoparticles (ZON) for the adsorption of Victoria Blue B dye from aqueous solution. Advanced Powder Technology 27(4), 1180-1188 (2016).
11. Zhag, Fan, Xiaoju Yin, and Weihua Zhang: Development of magnetic Sr5 (PO4) 3 (OH)/Fe3O4 nanorod for adsorption of Congo red from solution. Journal of Alloys and Compounds 657, 809-817 (2016).
12. Li, D. P., Zhang, Y. R., Zhao, X. X., & Zhao, B. X: Magnetic nanoparticles coated by aminoguanidine for selective adsorption of acid dyes from aqueous solution. Chemical engineering journal 232, 425-433 (2013).
13. Zhang, Randi: Adsorption of Congo red from aqueous solutions using cationic surfactant modified wheat straw in batch mode: kinetic and equilibrium study. Journal of the Taiwan Institute of Chemical Engineers, 45(5) 2578-2583 (2014).
14. HJ Rao, P King, YP Kumar, Equilibrium isotherm, kinetic modeling, and characterization studies of cadmium adsorption in an aqueous solution by activated carbon prepared from bauhinia purpurea leaves, Rasayan Journal of Chemistry, 2018.
15. M Ravikumar, P King, Equilibrium, kinetic and thermodynamic studies of congo red biosorption from textile wastewater using spathodea campanulata leaves. Rasayan Journal of Chemistry, 12(4) 2318-2327 (2019).
16. Venkata Rao Poiba, Bandela Sowjanya, Pulipati King & Meena Vangalapati (2023) Removal of methylene blue dye by using synthesised Grevillea robusta silver nanoparticles and optimisation of experimental parameters by response surface methodology (central composite design), Advances in Materials and Processing Technologies.
17. Gowthami V, Sowjanya B, Kumar MN, Vangalapati M. 2023. Synthesized MgO/Chitosan Nanocomposite: It's Application for the Removal of Dicofol and Optimization by Box Benhken Design. Nanoworld J 9(1): 1-7.